

Organic Ice Resist

Anpan Han, William Tiddi, Anna Elsukova, Marco Beleggia
DTU Danchip/Cen, Technical University of Denmark, Kgs. Lyngby, 2800 Denmark.

Introduction

A typical electron beam lithography (EBL) process (Fig. 1a) includes five steps: spin coating resists on samples with optically flat surfaces, baking, electron beam exposure, development, and sample drying. Focused electron-beam-induced deposition (FEBID, Fig. 1b), and ice lithography are examples of two other electron-beam-based nanopatterning methods. In FEBID, a gas is injected near the sample, and the gas molecules are adsorbed onto the sample surface. The adsorbed gas interacts with the electron beam, leading to the formation of a solid deposit on the sample surface. The ultimate resolution of this process is even better than EBL^[1, 2], and the lack of spin coating and development enables patterning to be applied on complex sample topographies to create 3D nanostructures^[3]. However, FEBID is very slow compared to EBL. In ice lithography^[4–6] (IL, Fig. 1c), water vapor condenses into a solid layer of ice that coats the sample held at cryogenic temperatures. IL allows nanopatterning on non-planar or fragile samples such as AFM tips and

carbon nanotubes. The patterning mechanism is so far unclear. Unfortunately, since most downstream nanofabrication instruments work at ambient conditions, the need for further in situ processing at cryogenic temperatures limits IL applications.

Recently, we discovered that frozen layers of simple organic molecules can be e-beam patterned for lithography applications. We adopted the term “organic ice resists” (OIR) for this process. The method is similar to additive manufacturing, also known as 3D printing^[7]; see also animation^[7]. We designed and built a custom apparatus^[8] that is more compact than the IL instrument^[5]. Our method is fundamentally different from prior art. It has striking advantages that complement established methods, while also enabling completely new applications. Specifically, as in IL and FEBID, we bypass the solvent development and drying needed in EBL. In strong contrast to IL, patterned OIR can be used ex situ for further characterization and processes. For thicker resists, our process is several orders of magnitude faster than FEBID.

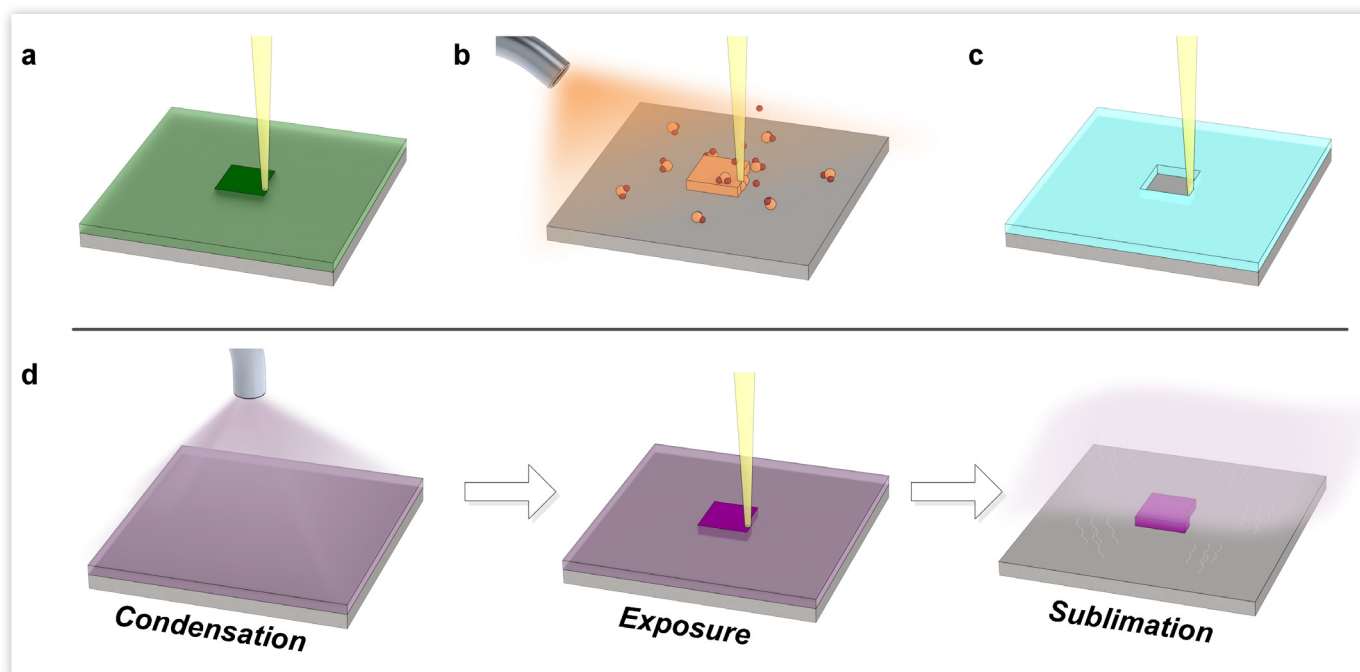


Figure 1: OIR patterning (d) compared to EBL (a), FEBID (b) and IL (c). Reprinted with permission from^[7]. Copyright {2017} American Chemical Society.

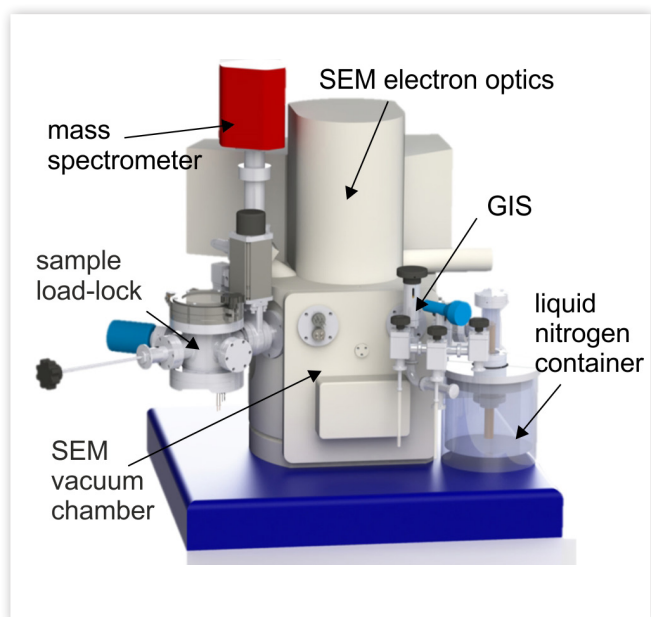


Figure 2: OIR instrument. The Zeiss SEM is modified with custom-made assemblies to accommodate the cryogenic operation and gas inlet needed to condense the organic vapors inside the chamber. Load lock is added for rapid sample exchange and ice sublimation. Reprinted with permission from [8]. Copyright {2018} Elsevier.

Instrumentation

Our OIR instrument (Fig. 2), inspired by the ice lithography system^[5], is based on a LEO SEM from Zeiss, which is equipped with an e-beam lithography attachment (Raith ELPHY Quantum). The detailed instrumentation and operation are reported in [8]. See also instrument operation and OIR processing video^[8]. On the exterior of the OIR instrument, we added a load lock chamber for sample transfer and warmup, and a gas injection system (GIS). Inside the SEM chamber, we added a cold finger and a cryostage, both cooled with liquid nitrogen. The sample holder surface measures 25 x 20 mm².

Results

To form the OIR film, we cool down the sample in the SEM vacuum and inject the organic gas through the GIS nozzle onto the cold sample surface, where it condenses to a uniform layer of organic ice. We irradiate the OIR thin film with the e-beam and then transfer the sample to the airlock, to heat it to room temperature while maintaining vacuum. A solid product is formed in the e-beam-exposed areas, whereas the unexposed OIR sublimates within minutes and is removed by the vacuum system of the airlock (Figure 1d). The resulting patterns are stable at ambient conditions. As in IL and FEBID, this sublimation step completely replaces

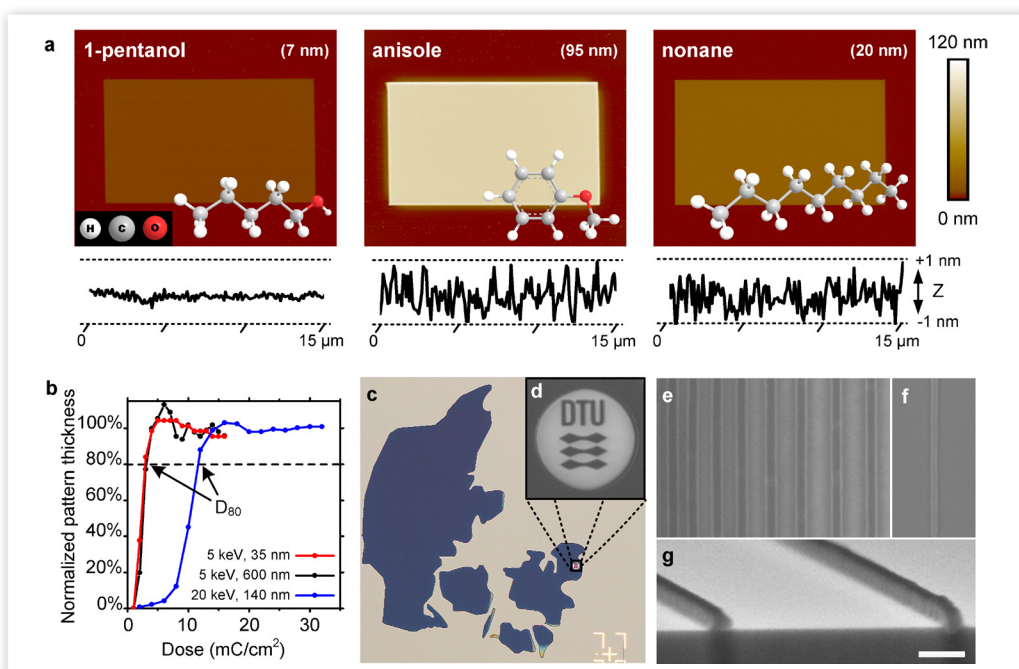


Figure 3. OIR patterns. (a) AFM images of 20 x 12 μm² rectangles patterned in OIR thin films and representative scan-lines across the rectangle surface. Average pattern thickness is in parentheses. (b) Contrast curves for nonane ice at 5 and 20 keV. The critical dose at 5 keV is unchanged even with a 20-fold time increase in thickness. (c, d) Large area map of Denmark made by exposed nonane ice (dark blue areas). The total exposure time was 75 min. The optical image (c) covers an area of 0.4 x 0.5 mm². The micrometric DTU logo (9 x 6 μm²) patterned in the Copenhagen region is visible in the SEM inset (d). (e) SEM image of 100-nm-wide lines patterned in nonane ice. (f) 60-nm-wide line patterned in anisole ice. (g) Tilted SEM view of patterned OIR lines reaching the edge of a 1 x 1 cm² chip. The OIR layer is uniform across the entire sample surface up to the very edge. Scale bar is 200 nm. Reprinted with permission from [7]. Copyright {2017} American Chemical Society.

the solvent development and drying needed in EBL. OIR involves no drying process, and hence no moving menisci, whose interfacial forces often destroy fragile samples. Unlike IL, our e-beam-patterned OIR can be used ex situ for further characterization and processing. The resulting patterns are equivalent to those made by a negative tone EBL resist.

The OIR thickness is controlled by adjusting the GIS leak valve and the total deposition time, and is proportional to the pressure drop in the GIS^[8]. The layers were condensed at substrate temperatures ranging from 120 K to 150 K without any observable difference in subsequent performances, indicating a robust process. The critical doses (D₈₀, Figure 3b) of

nonane (C_9H_{20}) ice for 5 and 20 keV e-beam exposures were reached at 3 and 12 mC / cm² respectively. The analysis of exposed thick layers revealed that OIR resist thickness does not affect the critical dose. This is in direct contrast to the gas-based FEBID method, which deposits matter monolayer by monolayer, resulting in a process time proportional to the volume of the deposited material. Although higher than for many EBL resists, the OIR dose is already ~100 times lower than in IL, allowing nanoscale fabrication as well as sub-mm features (Figure 3c–d) which would be prohibitively time-consuming using water ice. A benchmark figure for the FEBID dose required to deposit a single atomic monolayer from an organometallic precursor translates to 3 mC / cm²[9]. For OIR, the same dose can be used to pattern the 600-nm-thick OIR layers. Hence, OIR is up to ~1000 times faster than FEBID at depositing layers above 100-nm thickness. To investigate the resolution of OIR, we patterned and compared single line scans on OIR thin-films (Figure 3e–g) and on the negative-tone EBL resist AR-N 7520. We obtained OIR lines down to 60 nm wide and EBL resist lines 80 nm wide. The unexpectedly large EBL resist patterns indicate that feature size is currently limited by our custom instrument. To further probe the resolution performances of OIRs, we used a transmission electron microscope fitted with a gas cell and a cryostage to condense OIR layers on electron transparent membranes and perform analogous lithography experiments. The significantly improved feature size (down to 10 nm [7]) confirms that our SEM results are far from the ultimate resolution of this technique, and suggests that by improving our custom instrument we might achieve critical dimensions in line with EBL.

Another major advantage of OIR is 3D patterning capabilities using an iterative condense-exposure process (Fig. 4). The smallest features were 100 nm. Each OIR layer is 45 nm thick.

To create useful devices, lithographic patterns must be transferred into an underlying functional material. We used OIR patterns as etch masks

in reactive ion etching to create silicon nanostructures (Figure 5a-b). For nonane ice patterns, selectivity over silicon was 1:6, which is comparable to negative-tone EBL resists. Using oxygen plasma, we can remove the patterned OIR without leaving any residues or harming the underlying silicon.

One main advantage of OIR is that we can easily handle small samples such as the TEM membrane samples used in our TEM experiments. As a further demonstration, we patterned OIR onto diamond chips as small as 2 x 2 mm² to be used as etch masks (Figure 5c-e). Diamond substrates and nanopillars are used for purposes such as nitrogen-vacancy centers for quantum technology applications [10]. In contrast to EBL resist coating, uniform OIR layers of well-controlled thickness can easily be deposited on the entire sample surface, while the one-step lithography reduces sample manipulation to a minimum.

Future work

We aim to make OIR technology available to the scientific community. We are currently working with Raith to explore ways of implementing OIR as an add-on module for the eLINE Plus multitechnique EBL tool. If you are interested in OIR technology, please contact us or Raith's product management at sales@raith.com

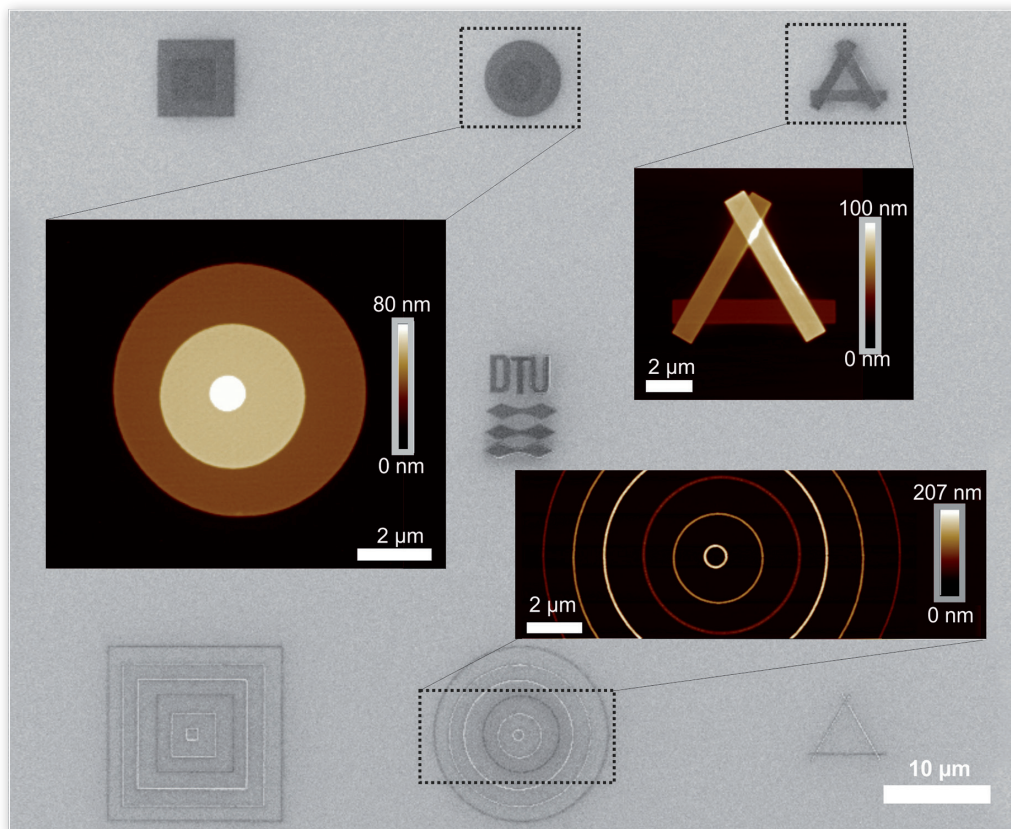


Figure 4. 3D OIR structures using 3 layers of OIR. Structures were made using a series of three CE cycles. The background image was taken with the SEM, and the magnified images were taken with the AFM. Each OIR layer is approximately 45 nm thick. The narrow lines have a total thickness of 135 nm, while the larger areas were under-exposed, resulting in a total thickness of 80 nm. Reprinted with permission from [8]. Copyright {2017} Elsevier.

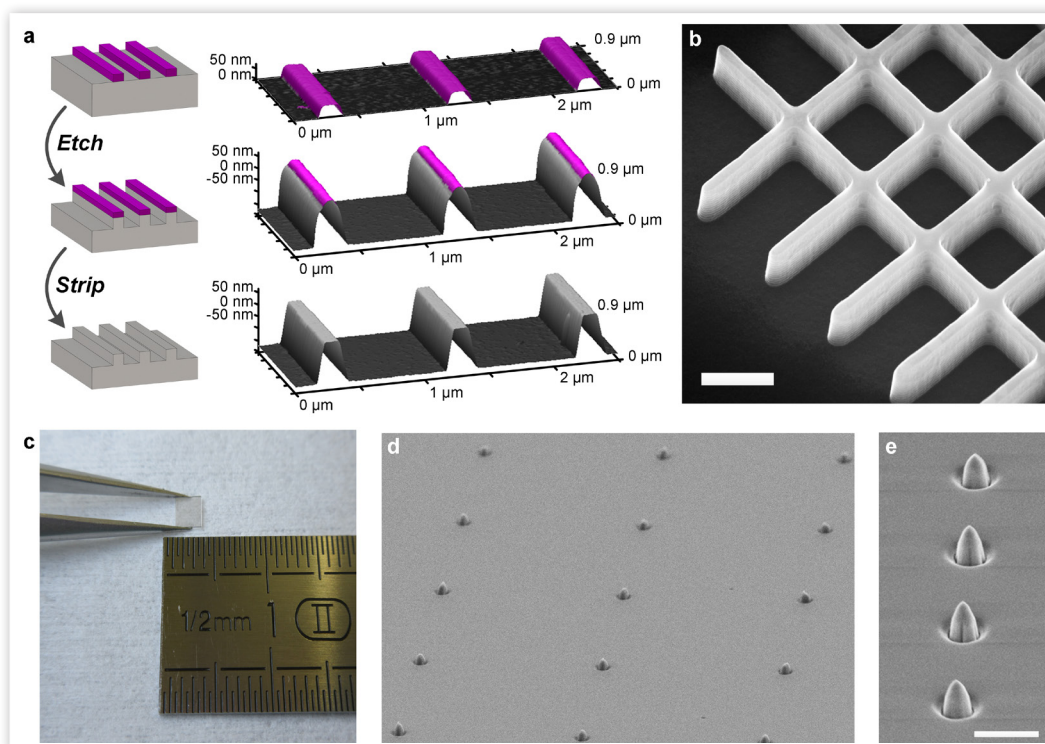


Figure 5. Fabrication of nanowires and nanopillars by plasma etching. (a) AFM profile evolution of OIR lines on a silicon substrate at three different steps in the etch process: as patterned, after silicon etch, and after removal of the residual OIR. Etch selectivity between the patterned OIR and silicon is 1:6. (b) SEM view of 400-nm-high silicon fins made using OIR and reactive ion etching. Scale bar is 500 nm. (c) Tweezers holding a 2 x 2 mm² diamond chip used for fabricating diamond quantum devices. (d) SEM view of an array (pitch 10 µm) of diamond nanopillars fabricated using patterned OIR as the etch mask. (e) Close-up of diamond pillars. Scale bar is 1 µm. Reprinted with permission from [7]. Copyright {2017} American Chemical Society.

References

- [1] J. C. van Oven, F. Berwald, K. K. Berggren, P. Kruit, and C. W. Hagen, "Electron-beam-induced deposition of 3-nm-half-pitch patterns on bulk Si," *J. Vac. Sci. Technol. B, Nanotechnol. Microelectron. Mater. Process. Meas. Phenom.*, vol. 29, no. 6, p. 06F305, 2011.
- [2] V. R. Manfrinato et al., "Resolution limits of electron-beam lithography toward the atomic scale," *Nano Lett.*, vol. 13, no. 4, pp. 1555–1558, 2013.
- [3] M. Esposito et al., "Nanoscale 3D chiral plasmonic helices with circular dichroism at visible frequencies," *ACS Photonics*, vol. 2, no. 1, pp. 105–114, 2015.
- [4] A. Han, D. Vlassarev, J. Wang, J. A. Golovchenko, and D. Branton, "Ice lithography for nanodevices," *Nano Lett.*, vol. 10, no. 12, pp. 5056–5059, 2010.
- [5] A. Han, J. Chervinsky, D. Branton, and J. A. Golovchenko, "An ice lithography instrument," *Rev. Sci. Instrum.*, vol. 82, no. 6, 2011.
- [6] A. Han, A. Kuan, J. Golovchenko, and D. Branton, "Nanopatterning on nonplanar and fragile substrates with ice resists," *Nano Lett.*, vol. 12, no. 2, pp. 1018–1021, 2012.
- [7] W. Tiddi, A. Elsukova, H. T. Le, P. Liu, M. Beleggia, and A. Han, "Organic Ice Resists," *Nano Letters* 2017 17 (12), 7886–7891, DOI: 10.1021/acs.nanolett.7b04190.
- [8] W. Tiddi, A. Elsukova, M. Beleggia, A. Han, "Organic ice resists for 3D electron-beam processing: instrumentation and operation" *Microelectronic Engineering*, Volume 192, 2018, Pages 38–43.
- [9] Hagen, C. W. *Appl. Phys. A*, 2014, 117, 1599–1605.
- [10] Babinec, T. M.; Hausmann, B. J. M.; Khan, M.; Zhang, Y.; Maze, J. R.; Hemmer, P. R.; Lončar, M. *Nature Nanotech.*, 2010, 5, 195–199.

Raith GmbH, Konrad-Adenauer-Allee 8, PHOENIX West, 44263 Dortmund, Germany
phone +49 231 / 95004 - 0, fax +49 231 / 95004 - 460, e-mail: sales@raith.com, website: www.raith.com

Raith America Inc., 1377 Long Island Motor Parkway, Suite 101, Islandia, New York 11749, USA
phone +1 631 738 9500, fax +1 631 738 2055, e-mail: sales@raithamerica.com

Raith Asia Ltd., Two Chinachem Exchange Square, No. 338 King's Road, Floor 11, Unit 03, North Point, Hong Kong
phone +852 2887 6828, fax +852 2887 6122, e-mail: sales@raithasia.com

Raith China Ltd., Room 1409, Tower B, Techart Plaza, No.30 Xue Yuan Road, Haidian District, 100083 Beijing, P.R.China
phone: +86 10 828679 22, fax: +86 10 828679 19, e-mail: sales@raithchina.com

Raith India Pvt. Ltd., Sri Krishna Complex, No 36, 2nd Floor, Opposite Mother Theresa School, M. E. S. Ring Road, Bangalore 560054, India
phone +91 80 2838 4949, Fax +91 80 2838 4949, e-mail: sales@raithindia.com